

Recent STAR results in high-energy polarized proton-proton collisions at RHIC

Bernd Surrow for the STAR Collaboration

Massachusetts Institute of Technology, 77 Massachusetts Avenue, Cambridge, MA 02139, USA

E-mail: surrow@mit.edu

Abstract. The STAR experiment at the Relativistic Heavy-Ion Collider at Brookhaven National Laboratory is carrying out a spin physics program in high-energy polarized $\vec{p} + \vec{p}$ collisions at $\sqrt{s} = 200 - 500$ GeV to gain a deeper insight into the spin structure and dynamics of the proton.

One of the main objectives of the spin physics program at RHIC is the extraction of the polarized gluon distribution function based on measurements of gluon initiated processes, such as hadron and jet production. The STAR detector is well suited for the reconstruction of various final states involving jets, π^0 , π^\pm , e^\pm and γ , which allows to measure several different processes. Recent results will be shown on the measurement of jet production and hadron production at $\sqrt{s} = 200$ GeV.

The RHIC spin physics program has recently completed the first data taking period in 2009 of polarized $\vec{p} + \vec{p}$ collisions at $\sqrt{s} = 500$ GeV. This opens a new era in the study of the spin-flavor structure of the proton based on the production of $W^{-(+)}$ bosons. Recent STAR results on the first measurement of W boson production in polarized $\vec{p} + \vec{p}$ collisions will be shown.

1. Introduction

The spin structure and dynamics of the nucleon is one of the fundamental and unresolved questions in Quantum Chromodynamics (QCD). Contrary to atomic physics where the total angular momentum of an atom can be accounted for by basic quantum theory in terms of its underlying atomic constituents, a complete theoretical description of the proton spin decomposed in terms of contributions from quark and gluon angular momenta and spins is still missing. Various experimental programs have been conducted in the past to deepen our understanding on the proton spin. Deep-inelastic scattering (DIS) experiments have clearly established that the quark spin contribution is small and accounts for only $\approx 25\%$ of the proton spin [1, 2].

High energy polarized $\vec{p} + \vec{p}$ collisions at $\sqrt{s} = 200 - 500$ GeV at RHIC provide a unique way to probe the proton spin structure and dynamics using hard scattering processes [3]. The production of jets and hadrons is the prime focus of the gluon polarization studies. The production of $W^{-(+)}$ bosons at $\sqrt{s} = 500$ GeV provides an ideal tool to study the spin-flavor structure of the proton. This has been pointed out at the very early design stages of the polarized proton collider program at RHIC [4].

The first global analysis of polarized DIS data, as well as results obtained by the PHENIX [5] and STAR [6] experiments in polarized $\vec{p} + \vec{p}$ collisions at RHIC placed a strong constraint on the gluon spin contribution in the gluon momentum range of $0.05 < x < 0.2$, and suggested that the gluon spin contribution is not large in that range [7]. Constraining the polarized gluon

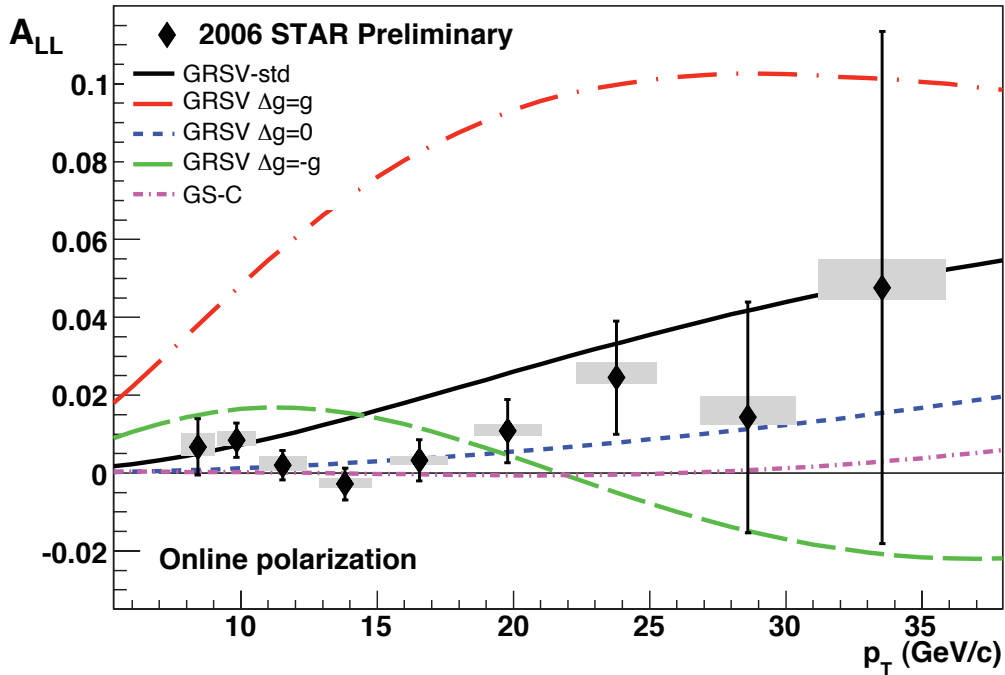


Figure 1. Recent STAR 2006 A_{LL} inclusive jet result.

distribution function, Δg , through inclusive measurements has been, so far, the prime focus of the STAR physics analysis program of the Run 3/4 [8], Run 5 [6] and Run 6 [9] data samples. Inclusive measurements, such as inclusive jet production, integrate over a fairly large x region for a given jet transverse momentum region. While those measurements provide a strong constraint on the value of Δg integrated over a range in x , those measurements do not permit a direct sensitivity to the actual x dependence. This motivates the need for correlation measurements in polarized $\vec{p} + \vec{p}$ collisions.

The STAR collaboration has presented a first measurement of the longitudinal spin transfer D_{LL} in inclusive Λ ($\Lambda \rightarrow p\pi^-$) and $\bar{\Lambda}$ ($\bar{\Lambda} \rightarrow \bar{p}\pi^+$) production in polarized proton-proton collisions at a center-of-mass energy of $\sqrt{s} = 200$ GeV [10]. This measurement may provide constraints on strange (anti) quark polarization [11] and can yield new insight into polarized fragmentation functions.

The first data taking period in 2009 of polarized $\vec{p} + \vec{p}$ collisions at $\sqrt{s} = 500$ GeV opens a new era in the study of the spin-flavor structure of the proton based on the production of $W^{-(+)}$ bosons. $W^{-(+)}$ bosons are produced predominantly through $\bar{u} + d$ ($u + \bar{d}$) collisions and can be detected through their leptonic decay. Quark and anti-quark helicity distribution functions are probed at large scales set by the mass of the W boson ($Q \sim m_W$) where theoretical calculations are well under control. The theoretical framework is well developed to describe the production of W bosons in high-energy polarized $\vec{p} + \vec{p}$ collisions including the description of the W decay leptons subject to experimental cuts, such as the transverse momentum p_T and pseudo-rapidity η of the final-state leptons [12, 13]. This development profits from a rich history of hadroproduction of weak bosons at the CERN SPS and the FNAL Tevatron and provides a firm basis to use W production as a new high-energy probe in polarized $\vec{p} + \vec{p}$ collisions [14].

The STAR Collaboration has provided critical measurements on the study of transverse spin effects in polarized $p + p$ collisions at RHIC. An overview of these results is discussed in a separate paper [15].

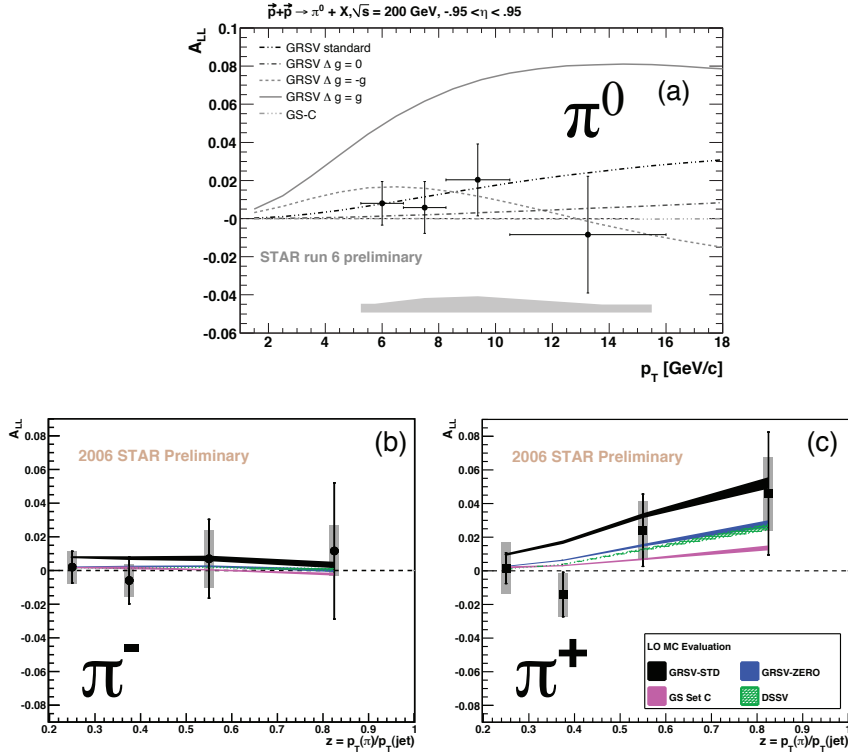


Figure 2. Recent STAR 2006 A_{LL} neutral pion result (a) and STAR 2006 A_{LL} results for charged pion (π^- and π^+) / jet correlation measurements (b/c).

2. Recent jet A_{LL} results

STAR reconstructs jets with the midpoint cone algorithm using clusters of charged track momenta measured with the STAR Time Projection Chamber (TPC) and tower energy deposits in the STAR Barrel Electromagnetic Calorimeter (BEMC) within a cone radius of $R \equiv \sqrt{\Delta\eta^2 + \Delta\phi^2}$ [9]. The jet sample was required to be within a fiducial range of $-0.7 < \eta_{\text{Detector}} < 0.9$ for the 2006 data sample with a cone radius of $R = 0.7$. The dominant fraction of jet events in the 2006 data sample are based on a jet patch (JP) trigger that required a minimum energy deposition for a group of towers over a region of $\Delta\eta \times \Delta\phi = 1.0 \times 1.0$. This trigger was taken in coincidence with a minimum-bias condition using the STAR Beam-Beam Counter (BBC).

Throughout the following discussion, four gluon polarization scenarios have been used as input to NLO perturbative QCD calculations of A_{LL} . The GRSV standard case refers to a global analysis fit of polarized DIS data [16]. The case for a vanishing gluon polarization (GRSV-ZERO) and the case of a maximally positive (GRSV-MAX) or negative (GRSV-MIN) gluon polarization have also been considered. The GS-C [17] set of Δg is reflected by a large positive gluon polarization at low x , a node around $x \sim 0.1$ and a negative gluon polarization at large x at a scale of $Q^2 \sim 1 \text{ GeV}^2$.

Figure 1 shows the most recent STAR preliminary result of A_{LL} for inclusive jet production as a function of p_T based on the 2006 data sample of 4.7 pb^{-1} . Typical beam polarization values during the 2006 data-taking period were 55 – 60%. The leading systematic uncertainty comes from the trigger and jet reconstruction biases. Differences between observed and true jet p_T are estimated using PYTHIA and GEANT simulations and result in corrections being applied to the jet p_T values. Additionally, the trigger conditions at STAR can artificially bias the analyzed data

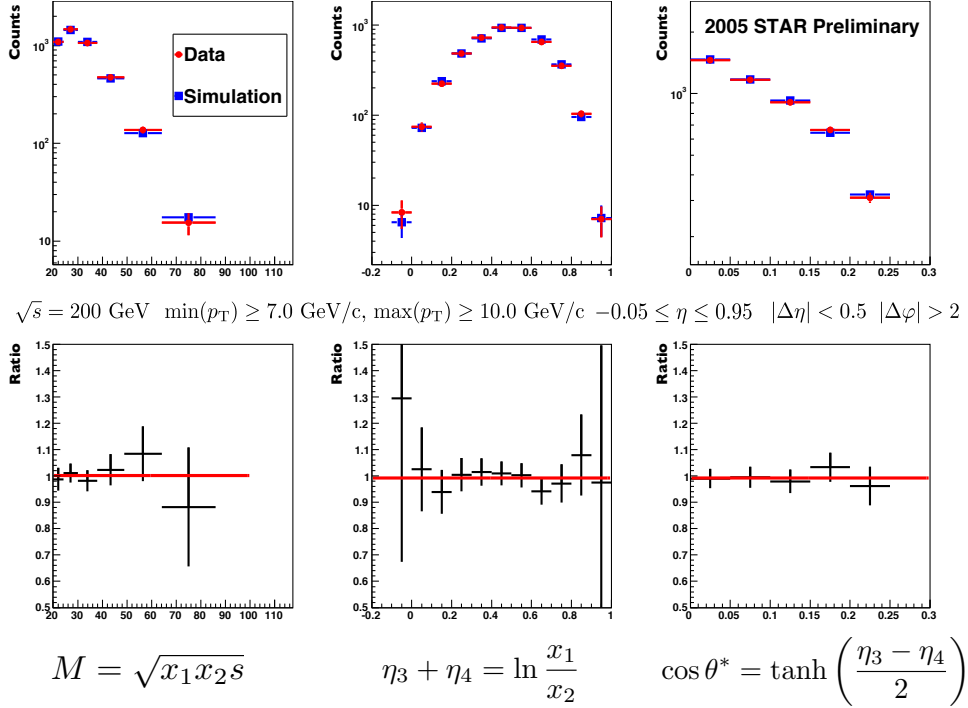


Figure 3. Comparison of STAR 2005 di-jet data and a PYTHIA Monte-Carlo showing the yield at the top and the ratio at the bottom for three characteristic di-jet variables (See text for further details).

sample towards particular flavors of partonic collisions. A conservative systematic uncertainty is evaluated to account for this effect which incorporates all allowable gluon polarization scenarios. The A_{LL} curves in Figure 1 are derived from NLO fits to world polarized DIS data by two separate theory groups, GRSV [16] and GS [17]. The currently measured result is consistent with a small gluon polarization scenario for the STAR x-range of $0.03 < x < 0.3$. This x-range accounts for $\sim 50\%$ of the total ΔG integral, i.e. $\Delta G = \int_0^1 \Delta g dx$, for GRSV-STD.

3. Recent neutral and charged pion A_{LL} results

Neutral pions are identified via the two-photon decay channel, which accounts for more than 98% of π^0 decays. Two primary sub-detectors, the STAR Barrel Electromagnetic Calorimeter (BEMC) and respective Shower Maximum Detector (SMD) are employed to reconstruct decay photons from mid rapidity neutral pions. Charged pion production is of particular interest since the difference of the longitudinal double-spin asymmetries for π^+ and π^- production, $A_{LL}(\pi^+) - A_{LL}(\pi^-)$, tracks the sign of Δg , due to the opposite signs of the polarized distribution functions for up and down quarks. The STAR Time Projection Chamber (TPC) offers robust reconstruction and identification of charged pions up to a transverse momentum of 15 GeV/c. Particle identification is accomplished using measurements of ionization energy loss in the TPC.

Figure 2 (a) shows A_{LL} for neutral pion production at mid rapidity as a function of p_T based on the 2006 data sample [18]. This new measurement is shown in comparison to NLO calculations assuming different gluon polarization scenarios [9, 18]. This measurement reaches to higher p_T values compared to previous measurements by PHENIX [19] and STAR [20]. At the present level of precision, the data excludes extreme gluon polarization scenarios. The STAR collaboration has recently presented also results for neutral pion production at forward rapidity

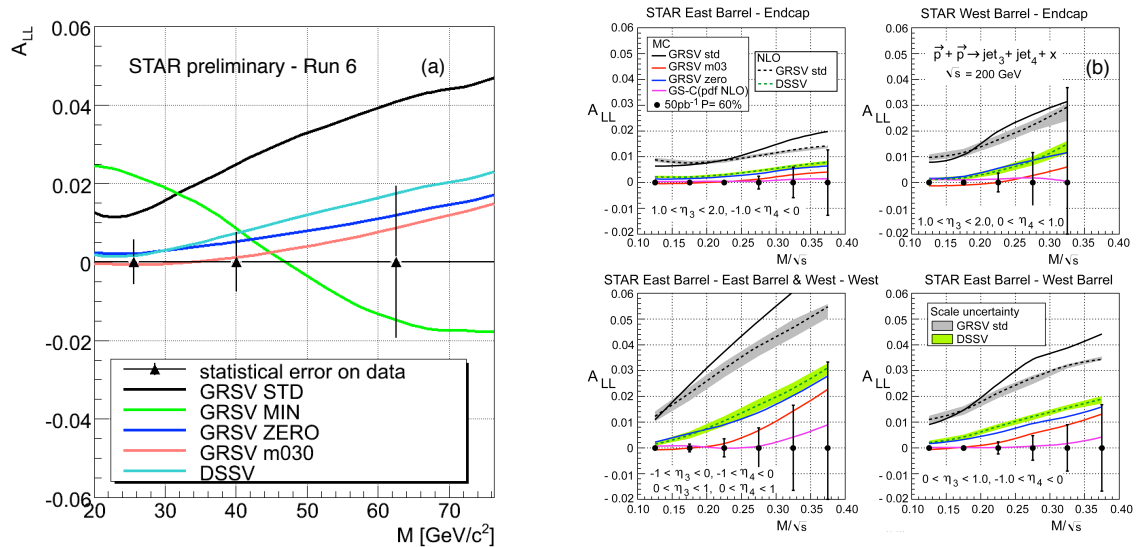


Figure 4. (a) Statistical precision of the longitudinal double-spin asymmetry, A_{LL} , as a function of the di-jet invariant mass, M , for the 2006 RHIC data sample. (b) Longitudinal double-spin asymmetry, A_{LL} , for di-jet production as function of the ratio M/\sqrt{s} for different topological combinations of the STAR BEMC and the STAR EEMC acceptance region.

based on the STAR Electromagnetic Endcap Calorimeter (EEMC) and the STAR Forward Pion Detector (FPD) [21]. These measurements provide an important milestone for future photon-jet coincidence measurements at STAR.

Figure 2 (b) and (c) show STAR's new preliminary result of A_{LL} for charged pion (π^- and π^+) / jet correlation measurements at mid rapidity. Charged pions are reconstructed opposite a jet that triggered the experiment. The data are shown versus $z \equiv p_T(\pi)/p_T(\text{jet})$ and were obtained in 2006 [22]. Full NLO calculations for this observable have recently been released [23]. These calculations will provide the basis for charged pion results to be included in a global analysis. The data shown for charged pion production are compared to a LO MC evaluation of A_{LL} excluding extreme scenarios of Δg . The measurement of $A_{LL}(\pi^+)$ is of particular interest, since its analyzing power is large because of the large ug scattering contribution to the production cross section and sizable $\Delta u/u$. In the future, more precise measurements of $A_{LL}(\pi^+)$ have a great potential for providing a better understanding of Δg .

4. Status and prospects of di-jet production

Correlation measurements such as those for di-jet production allow for a better constraint of the partonic kinematics and thus the shape of Δg . At LO, the di-jet invariant mass, M , is proportional to the product of the x values of the partons, $M = \sqrt{s}\sqrt{x_1x_2}$, whereas the pseudo-rapidity sum of the final-state jets, $\eta_3 + \eta_4$, is proportional to the logarithm of the ratio of the x values, $\eta_3 + \eta_4 = \ln(x_1/x_2)$. Photon-jet coincidence measurements are expected to provide a theoretically clean way to extract Δg . A LO extraction of Δg alone would allow a model-independent way to constrain the x dependence, which would be an important contribution, without making an a priori assumption on the functional form of Δg as is currently required in a global analysis. Measurements at both $\sqrt{s} = 200$ GeV and $\sqrt{s} = 500$ GeV are preferred to maximize the kinematic reach in x and possibly provide a means to observe effects of scaling violations at fixed x by measuring different p_T values. The wide acceptance of the STAR experiment permits reconstruction of di-jet events with different topological configurations,

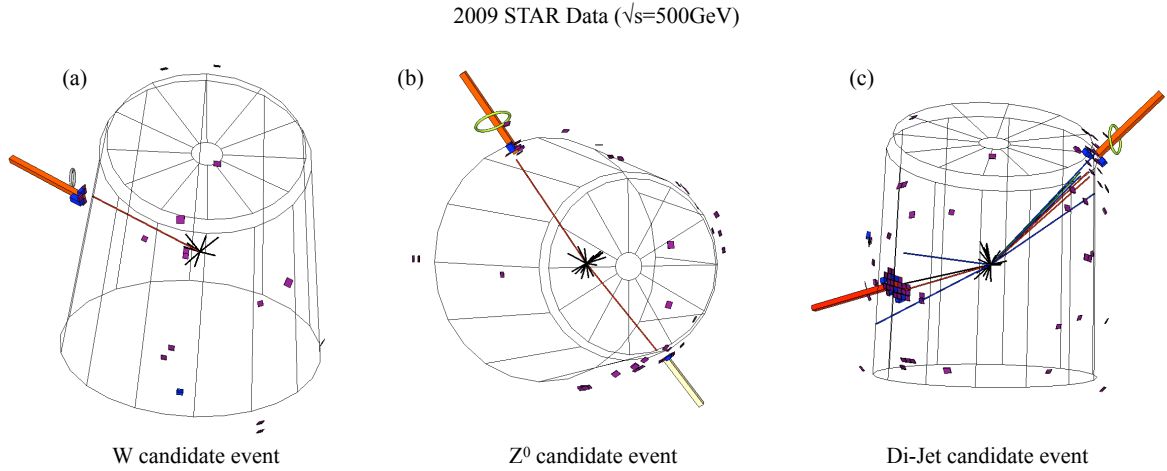


Figure 5. Event displays from the 2009 data taking period at $\sqrt{s} = 500 \text{ GeV}$ showing a W candidate event (a), a Z^0 candidate event and a di-jet candidate event (c).

i.e. different η_3/η_4 combinations, ranging from symmetric ($x_1 = x_2$) partonic collisions to asymmetric ($x_1 < x_2$ or $x_1 > x_2$) partonic collisions. This, together with the variation of the center-of-mass energy, is expected to constrain Δg over a wide range in x of approximately $\sim 2 \cdot 10^{-3} < x < 0.3$ for di-jet and photon-jet events. The NLO framework for correlation measurements exists and therefore those measurements can be used in a global analysis [24].

Figure 3 shows a comparison of STAR 2005 di-jet data and a PYTHIA Monte-Carlo simulation with the yield at the top and the ratio at the bottom for the invariant mass M , the pseudo-rapidity sum $\eta_3 + \eta_4$ and the cosine of the partonic center-of-mass scattering angle $\cos \theta^*$ determined from the pseudo-rapidities of both final-state jets. The normalization between data and Monte-Carlo is fixed by the invariant mass distributions. The same normalization factor is then applied to both other di-jet distributions. Data and Monte-Carlo are found to be in good agreement.

Figure 4 (a) shows the statistical precision of the longitudinal double-spin asymmetry, A_{LL} , as a function of the di-jet invariant mass, M . Those uncertainties, extracted from the 2006 data sample, are compared to a LO MC evaluation of A_{LL} computed with a PYTHIA MC sample using different event weights to account for different polarized gluon distribution functions of GRSV [16] and DSSV [7]. The size of the statistical uncertainty at the highest invariant mass bin is at the level of the difference between GRSV-STD and DSSV.

Figure 4 (b) shows the expected precision for the longitudinal double-spin asymmetry, A_{LL} , for di-jet production as a function of M/\sqrt{s} for different topological combinations of the STAR BEMC and the STAR Endcap Electromagnetic Calorimeter (EEMC) acceptance regions. Taking into account the different η ranges covered, and equivalently, the different $\cos \theta^*$ regions being probed, each panel represents a different range in x_1/x_2 . At LO, $\cos \theta^*$ amounts to $\tanh\left(\frac{\eta_3 - \eta_4}{2}\right)$. The upper left panel effectively probes asymmetric partonic collisions where predominantly a low- x gluon collides with a high- x quark at large invariant masses. The effective variation of x_1 and x_2 amounts to $0.2 < x_1 < 0.6$ and $0.07 < x_2 < 0.2$. In contrast, a kinematic region of larger x values is probed at predominantly symmetric partonic collisions such as the one shown in the lower right panel. The effective variation of x_1 and x_2 is roughly equal and given by the horizontal axis of the lower right panel. The projected uncertainties are shown for a luminosity of 50 pb^{-1} and a beam polarization of 60%. Those projected uncertainties are compared to a LO

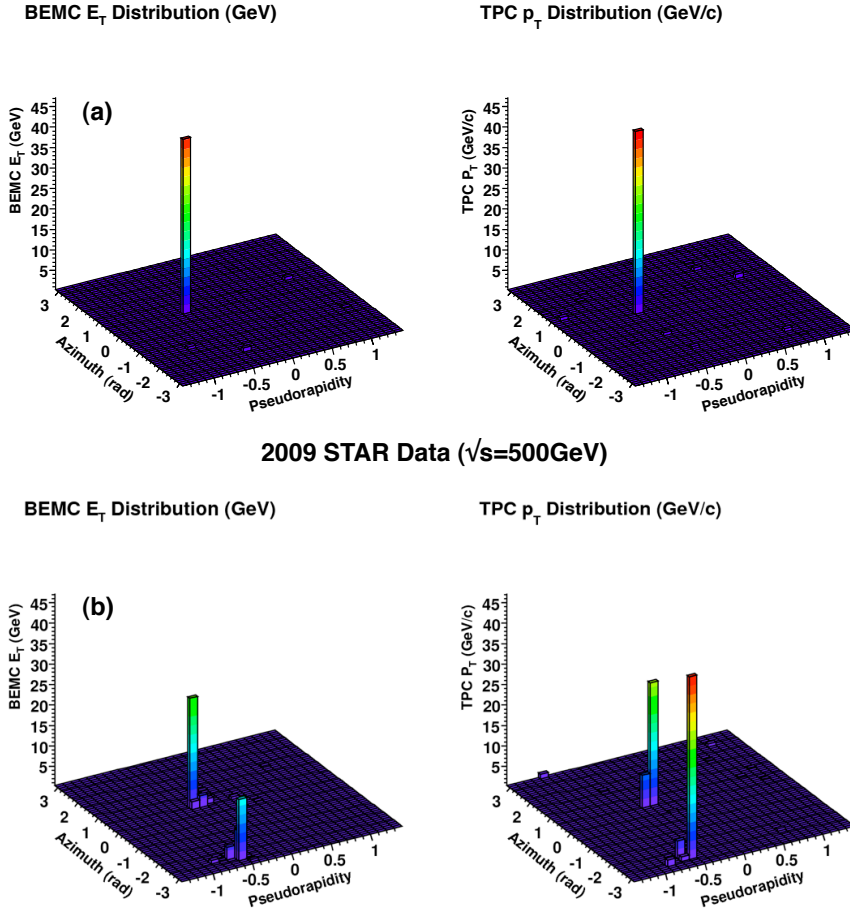


Figure 6. Lego plot showing the BEMC E_T and the TPC p_T distribution for a W candidate event (a) and a di-jet candidate event (b).

evaluation of A_{LL} and a full NLO A_{LL} calculation. Scale uncertainties are shown as a shaded band for DSSV and GRSV-STD reflecting a variation of the invariant mass M as a hard scale of $2M$ and $0.5M$. Asymmetric cuts are imposed for the LO MC and the NLO determination of $\min(p_T) \geq 7 \text{ GeV}/c$ and $\max(p_T) \geq 10 \text{ GeV}/c$. The result of a LO MC evaluation using GS-C [17] for Δg is also shown. GS-C is still consistent with the current inclusive jet results [9]. A cone radius of $R = 0.7$ has been used. Good agreement is found between a LO MC evaluation of A_{LL} and a full NLO calculation. Scale uncertainties are found to be small in comparison to the variation of the chosen polarized gluon distribution functions, in particular, at large values of M .

While inclusive measurements from STAR have provided important constraints on Δg , and will continue to do so, the impact of correlation measurements to the x dependence should greatly enhance our understanding of Δg .

5. Measurement of W boson production at STAR

The data used for the first W boson production analysis at STAR were collected in 2009 colliding polarized proton beams at 250 GeV. The STAR detector systems used in this analysis are the STAR Time Projection Chamber (TPC), the STAR Barrel Electromagnetic Calorimeter

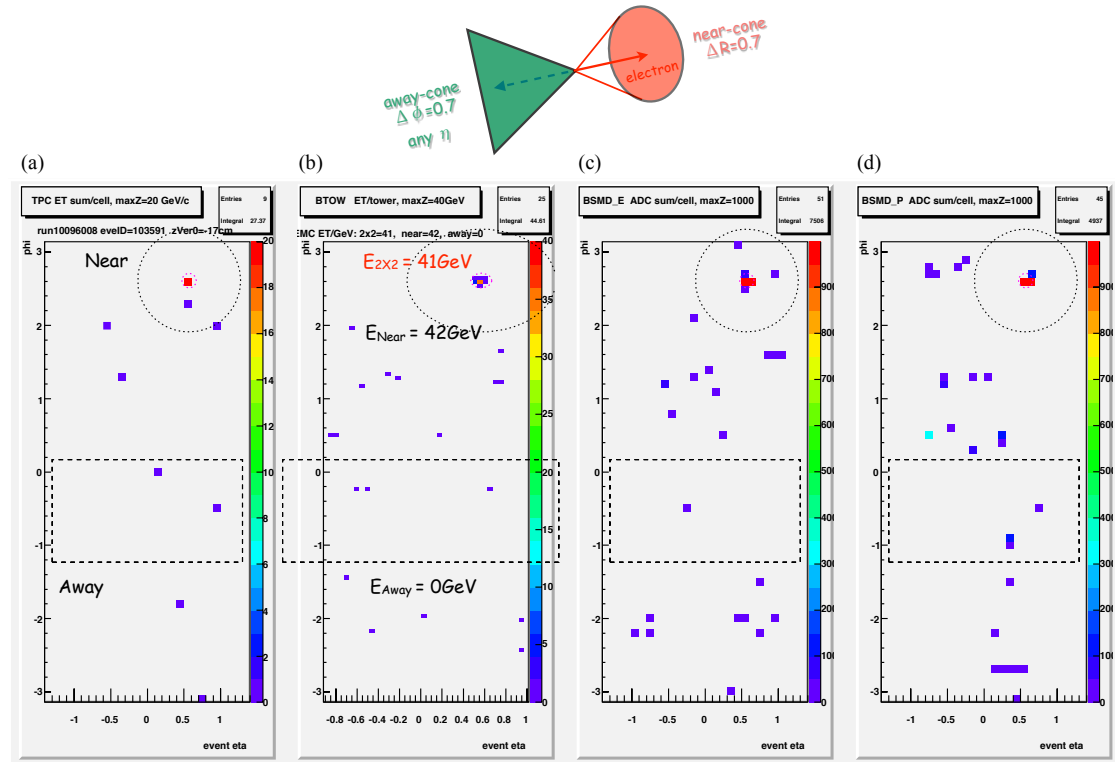


Figure 7. Illustration of the W offline selection criteria (top) and the distribution of the TPC p_T (a) the BEMC E_T (b) and both BEMC SMD layers (c) / (d) in azimuth and pseudo-rapidity.

(BEMC) and STAR Electromagnetic Endcap Calorimeter (EEMC). Only their tower response has been taken into account in this analysis. The BEMC was used to measure the transverse energy, E_T , of e^\pm . The suppression of the QCD background by several orders of magnitude was based on the TPC, BEMC and EEMC. Figure 5 shows event displays from the 2009 data taking period for a W candidate event (a), a Z^0 candidate event and a di-jet candidate event (c). A lego plot is shown in Figure 6 displaying the BEMC E_T and the TPC p_T distribution for a W candidate event at the top and a di-jet candidate event at the bottom.

Proton-proton collision events focusing on W production at $\sqrt{s} = 500$ were identified by a two-step energy requirement in the BEMC. Electrons and positrons from W production at mid rapidity are characterized by large E_T peaked at $\sim M_W/2$ (Jacobian peak). At the hardware trigger level (L0), a high tower (HT) calorimetric trigger condition required $E_T > 7.3$ GeV in a single BEMC tower. At the software trigger level (L2), a dedicated trigger algorithm was developed that required that a 2×2 tower cluster E_T sum exceeds 13 GeV. The offline selection of W candidate events is based on kinematical and topological difference between leptonic W^\pm decays, and QCD background events as shown in Figure 5 and Figure 6. Events from $W^\pm \rightarrow e^\pm + \nu$ decays contain a nearly isolated e^\pm with a neutrino in the opposite direction in azimuth. The neutrino escapes detection, leading to a large missing energy.

Figure 7 illustrates the basic idea of the selection of W candidate events. The 2D histograms show for one W candidate event the TPC p_T (a) and the BEMC tower E_T (b) distribution along with both BEMC shower-maximum detector (SMD) layers (c) / (d) as a function of the azimuthal angle ϕ and the pseudo-rapidity η . The approximate area of a 2×2 tower cluster is indicated by a small circle around the large energy deposition in a single BEMC tower. Also shown is the size of a cone (near-cone) around the electron candidate. The away-side area

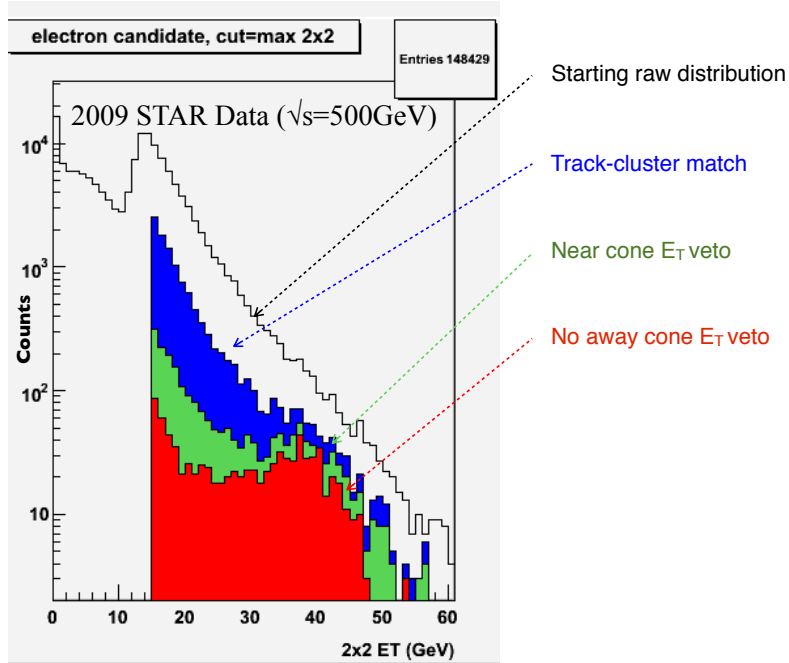


Figure 8. Evolution of W offline selection cuts (See text for further details).

is sketched by the black dashed rectangular region. The TPC high- p_T entry appears in the same $\eta - \phi$ region as the large BEMC E_T entry. Both BEMC SMD layers show a large energy deposition at the same location in the $\eta - \phi$ plane as the TPC high- p_T and the BEMC high- E_T entry. An electron candidate is defined to be any TPC track with $p_T > 10 \text{ GeV}/c$ that is associated with a primary vertex with $|z| < 100 \text{ cm}$, where z is the distance along the beam direction. A 2×2 BEMC tower cluster E_T sum is required to be larger than 15 GeV. The excess BEMC E_T sum in a 4×4 tower cluster centered around the respective 2×2 tower cluster is required to be below 5%. In addition, the distance between the 2×2 cluster tower centroid and the TPC track is required to be less than 7 cm. A near-cone is formed around the electron candidate direction with a radius in $\eta - \phi$ space of $R = 0.7$. The excess BEMC and TPC E_T sum is required to be less than 12% of the 2×2 cluster E_T . The away side requirement is based on a cut on the BEMC and TPC E_T sum to be less than 8 GeV. This sum is extended over the full η range of the BEMC and EEMC and $\Delta\phi = 0.7$ as shown in Figure 7. Figure 8 shows the evolution of all cuts for the BEMC 2×2 E_T distribution. A clear Jacobian peak emerges characteristic for W production in contrast to QCD background dominating the low E_T region.

A data-driven procedure was applied to estimate the level of QCD background events. The first part consists of an estimate of the impact of the missing calorimeter coverage for $-2 < \eta < -1$ on the cluster E_T distribution. This estimate was obtained by performing a parallel analysis without the EEMC as an active detector. The difference in yield of accepted events as a function of E_T provides an absolute estimate for the missing calorimetric coverage. The remaining background is estimated by fitting a separate QCD shape distribution in E_T to the region of $E_T < 19 \text{ GeV}$ shown as the black histogram in Figure 9. The fitted QCD background distribution is shown by the blue histogram in Figure 9. The background subtracted distribution is shown by the yellow histogram. Figure 9 also shows the distribution from a PYTHIA Monte-Carlo simulation. Good agreement in yield and shape is found between the data and Monte-Carlo distribution for the charge-sum BEMC E_T distribution. In the meantime, a considerable

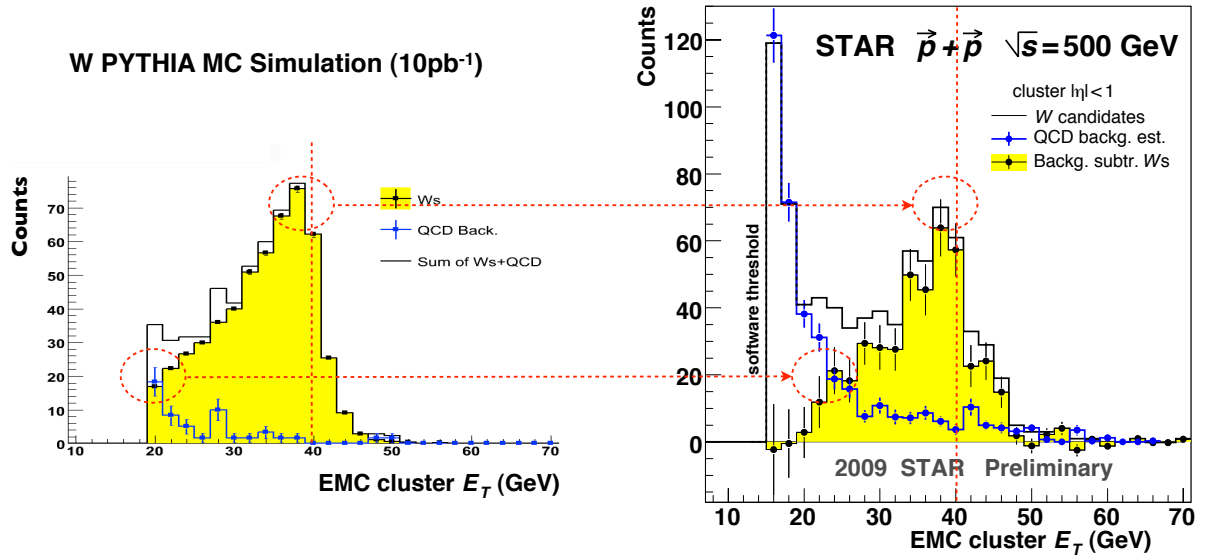


Figure 9. Reconstructed BEMC lepton transverse energy for W events.

effort has been performed on the TPC calibration to allow a full charge-sign separation. This and in particular the first measurement of the respective charge-separated cross-sections and parity-violating single-spin asymmetries A_L at mid rapidity will be discussed in a forthcoming publication.

Future planned high-statistics measurements at forward and backward pseudo-rapidities will focus on constraining the polarization of \bar{d} and \bar{u} quarks, respectively to deepen our understanding of the spin structure of the QCD sea.

References

- [1] Ashman J *et al.* (EMC) 1989 *Nucl. Phys.* **B328** 1
- [2] Filippone B W and Ji X D 2001 *Adv. Nucl. Phys.* **26** 1
- [3] Bunce G, Saito N, Soffer J and Vogelsang W 2000 *Ann. Rev. Nucl. Part. Sci.* **50** 525
- [4] Underwood D *et al.* 1992 *Part. World.* **3** 1–12
- [5] Adare A *et al.* (PHENIX) 2007 *Phys. Rev.* **D76** 051106
- [6] Abelev B I *et al.* (STAR) 2008 *Phys. Rev. Lett.* **100** 232003
- [7] de Florian D, Sassot R, Stratmann M and Vogelsang W 2008 *Phys. Rev. Lett.* **101** 072001
- [8] Abelev B I *et al.* (STAR) 2006 *Phys. Rev. Lett.* **97** 252001
- [9] Sarsour M *et al.* (STAR) 2008 *Proceedings of the 18th International Spin Physics Symposium*
- [10] Abelev B I *et al.* (STAR) 2009 *Phys. Rev.* **D80** 111102
- [11] Xu Q h, Liang Z t and Sichtermann E 2006 *Phys. Rev.* **D73** 077503
- [12] Nadolsky P M and Yuan C P 2003 *Nucl. Phys.* **B666** 31–55
- [13] de Florian D and Vogelsang W 2010 (*Preprint 1003.4533*)
- [14] Kotwal A V and Stark J 2008 *Ann. Rev. Nucl. Part. Sci.* **58** 147–175
- [15] Eun L *et al.* (STAR) 2010 *Proceedings of the 26th Winter Workshop on Nuclear Dynamics*
- [16] Gluck M, Reya E, Stratmann M and Vogelsang W 2001 *Phys. Rev.* **D63** 094005
- [17] Gehrmann T and Stirling W J 1996 *Phys. Rev.* **D53** 6100–6109
- [18] Hoffman A *et al.* (STAR) 2008 *Proceedings of the 18th International Spin Physics Symposium*
- [19] Adare A *et al.* (PHENIX) 2009 *Phys. Rev. Lett.* **103** 012003
- [20] Abelev B I *et al.* (STAR) 2009 *Phys. Rev.* **D80** 111108
- [21] Wissink S *et al.* (STAR) 2008 *Proceedings of the 18th International Spin Physics Symposium*
- [22] Kocoloski A *et al.* (STAR) 2008 *Proceedings of the 18th International Spin Physics Symposium*
- [23] de Florian D 2009 *Phys. Rev.* **D79** 114014
- [24] de Florian D, Frixione S, Signer A and Vogelsang W 1999 *Nucl. Phys.* **B539** 455–476